HHS Public Access

Author manuscript

Ocul Surf. Author manuscript; available in PMC 2021 October 01.

Published in final edited form as:

Ocul Surf. 2020 October ; 18(4): 857–864. doi:10.1016/j.jtos.2020.09.002.

Activation of Ocular Surface Mast Cells Promotes Corneal Neovascularization

WonKyung Cho, **Sharad K Mittal**, **Elsayed Elbasiony**, **Sunil K Chauhan**

[1]Schepens Eye Research Institute of Mass Eye and Ear, Harvard Medical School, Boston, MA, USA

Abstract

Purpose: Mast cells, historically known for their effector function in the induction of allergic diseases, reside in all vascularized tissues of the body in particular proximity to blood and lymphatic vessels. As neighboring sentinel cells to blood vessels, mast cells have been associated with angiogenesis. Here we assess the direct contribution of mast cells to neovascularization at the ocular surface.

Methods: Corneal neovascularization was induced by placing a single figure-of-eight intrastromal suture 1 mm from the limbus in mast cell-deficient ($cKit^{W\text{-}sh}$), C57BL/6, and Balb/c mice. Corneas were harvested at 6h post-suture to quantify $cKit^{+}Fc\varepsilon R1^{+}$ mast cells using flow cytometry and tear wash was collected within 6h to measure β-hexosaminidase and tryptase. Neovascularization was assessed using slit-lamp biomicroscope and immunohistochemistry analysis of corneas harvested on day 4 post-suture. To investigate the effects of mast cells on blood vessel growth, mast cells were co-cultured with vascular endothelial cells (VECs), and tube formation and proliferation of VECs were measured. 2% cromolyn was administered locally to inhibit mast cell activation *in vivo*.

Results: Placement of corneal suture activates ocular surface mast cells which infiltrate into the cornea adjacent to new vessels. Mast cell-deficient mice develop significantly fewer new vessels following suture placement. Mast cells directly promote VEC proliferation and tube formation, partly through secreting high levels of VEGF-A. Pharmacological inhibition of mast cell activation results in significantly less corneal neovascularization.

Conclusion: Our data demonstrate that ocular surface mast cells are critical to corneal neovascularization, suggesting mast cells as a potential therapeutic target in the treatment of corneal neovascularization.

Corresponding author: Sunil Chauhan, DVM, PhD., Schepens Eye Research Institute of Mass Eye and Ear, Harvard Medical School, 20 Staniford Street, Boston, MA 02114 | sunil_chauhan@meei.harvard.edu| Phone: 617-912-0258; Fax: 617-912-0117.

Author contributions:

W.C. assisted in designing the study, performed *in vivo* and *in vitro* experiments, analyzed the data, and wrote the manuscript. S.K.M. assisted in designing experiments, analyzed the data, and wrote the manuscript. E.E. assisted in performing *in vivo* experiments. S.K.C. contributed the underlying hypothesis, designed the study, analyzed data, and wrote the manuscript.

Disclosure/conflicts of interest: The authors have no financial conflict of interest. This work was supported by the National Institutes of Health grants R01EY029727 and P30EY003790.

Introduction

The cornea exhibits a unique quality of being a completely avascular tissue, which is maintained by a dynamic balance between angiogenic and anti-angiogenic factors [1]. In inflammatory, traumatic, or infectious disorders, this homeostasis equilibrium is disrupted, resulting in neovascularization that can lead to marked vision impairment or even complete loss of vision [2, 3]. Neovascularization, pathological growth of new vascular structures, is typical not only in ocular surface disorders but in tumors and other inflammatory disorders [4, 5]. As such, there is considerable interest in understanding the underlying mechanism of neovascularization, including the contribution of immune cells that primarily reside in the close proximity to blood vessels such as mast cells [6, 7].

Mast cells are tissue-resident immune cells, distributed throughout vascularized tissues in the body that congregate around blood and lymph microvessels and nerve endings [6–8]. Mast cells are often termed the sentinel cells as they reside, particularly in abundance at surfaces that interface with the outside environment (e.g., skin, airways, and gastrointestinal tract) [8]. Mast cells upon activation release preformed and *de novo* synthesized inflammatory mediators into the extracellular environment [9, 10]. These mediators include various cytokines, growth factors, enzymes, and vasoactive amines [6, 9]. Apart from their well-established role as effector cells in eliciting IgE-mediated allergic response, mast cells have been implicated in a much broader spectrum of inflammatory disorders, including cancer and arthritis [11, 12]. We have previously reported that mast cells contribute to non-allergic ocular conditions, including inflammatory haze and graft rejections [13, 14]. Given their close proximity to blood vessels, mast cells have been linked with angiogenesis [6]. However, the majority of the studies on mast cell-mediated angiogenesis have been limited to tumor biology [15, 16].

In the current study, we conducted a series of novel experiments to determine how non-IgE mediated activation of mast cells promote neovascularization and to uncover the underlying mechanism involved. We investigated the function of mast cells using a well-characterized murine model of inflammatory corneal neovascularization [17]. Here, using genetic and pharmacological inhibition of mast cells, we report for the first time that mast cell deficiency leads to reduced corneal neovascularization. Furthermore, we demonstrate that mast cells secrete high levels of VEGF-A and directly promote vascular endothelial cell proliferation and tube formation.

Materials and Methods

Animals

Six- to eight-week-old BALB/c and C57BL/6 wild-type and mast cell-deficient cKit$^{w\text{-}sh}$ mice (Stock No: 012861) were purchased from Jackson Laboratory, Bar Harbor, ME for the described experiments. The mice were housed in the Schepens Eye Research Institute animal vivarium and treated according to the Use of Animals in Ophthalmic and Vision Research guidelines set forth by the Association for Research in Vision and Ophthalmology.

All protocols were approved by the Animal Care and Use Committee of Schepens Eye Research Institute.

Corneal Neovascularization Model

Corneal neovascularization was induced by placing a single intrastromal suture on anesthetized mice, as previously described [18]. Briefly, a single figure-of-eight suture was intrastromally placed on the nasal side of the cornea, 1.0 mm from the limbal area using 11.0 nylon sutures (MANI, Tochigi, Japan). Following suture placement, a triple antibiotic ointment was applied topically. Mice were administered a subcutaneous injection of buprenorphine to mitigate suture-induced pain. Ocular surface tear wash (5 μL/wash) was collected at 0, 1, 3, and 6h post-suture placement and pooled together to measure mast cell activation. Mice were clinically assessed using a slit lamp, and subsequently, on day 4 were euthanized and their corneas (including the limbus) were harvested for further analysis.

Mast cell inhibitor administration

Three microliters of PBS or 2% sodium cromolyn in PBS (Sigma-Aldrich Corp., St. Louis, MO, USA) were administered topically to sutured corneas at five-time points on the day of suture placement (−3, −1, 0, and 1 and 3 hours postoperatively). Furthermore, PBS or cromolyn was administered topically 4x/day (every 3 hours) and 1x/day via subconjunctival injection in the evening. Five μL of PBS or 2% cromolyn was injected on the temporal subconjunctiva to prolong the blockade of mast cell activation overnight.

Corneal Tissue Isolation and Digestion

Single-cell suspensions were prepared from corneas, as previously described [19, 20]. Briefly, corneas were digested in RPMI media (Lonza, Walkersville, MD, USA) containing 4 mg/mL collagenase type IV (Sigma-Aldrich, St. Louis, MO) and 2 mg/mL DNase I (Roche, Basel, Switzerland) for 45 minutes at 37°C. Following this, cells were filtered through a 70-μm cell strainer.

Cell Culture Assays

Mast cells were generated by culturing bone marrow cells in the presence of stem cell factor (SCF; 50 ng/mL) and IL-3 (10 ng/mL) for 3 to 4 weeks. The culture media was changed every 3 to 4 days. This method of cell culture generates a mast cell population of >90% purity (Fig. S1). For the mast cell stimulation assays, mast cells were cultured either in medium alone or were stimulated with 1 ng/ml concentration of IL-33 (Biolegend, CA, USA) for 24 hours at 37°C. The cells were harvested for co-culture assays and to measure VEGF-A levels using methods described below.

MS-1 cell line, generated from microvessels of murine endocrine pancreas, has previously been used to study microvascular endothelial cell-mediated angiogenesis [21, 22]. MS-1 cells were maintained in a monolayer culture in endothelial cell basal medium-2 supplemented with growth factors [5% FBS, VEGF, FGF, EGF, IGF] at 37°C in 5% CO2-containing humidified air.

Tube formation assay

A Matrigel assay was set up in a flat-bottomed 96-well plate in triplicates as previously described [23]. In brief, MS1 (a mouse pancreatic endothelial cell line) were trypsinized, counted and resuspended in EBM-2 basal medium (Lonza, USA). Matrigel basement membrane (Millipore, MA, USA) was plated into each well (100 μl/well) and incubated for 1 hour at 37°C until adequate polymerization. Next, 2×10^4 VECs (MS1) were co-cultured in basal media alone, with supplemented growth factors [5% FBS, VEGF, FGF, EGF, IGF] (EGM-2MV endothelial cell growth medium; Lonza, USA) or with 2×10^4 mast cells (stimulated with 1 ng/ml IL-33 for 24 hrs) (1:1 ratio; 100 μl/well) on the matrigel surface, and was incubated at 37°C.Tube formation was observed for 12 hours, and micrographs of co-cultures were captured using an inverted brightfield microscope (Leica).

Proliferation assay

VEC proliferation was measured using the BrdU proliferation kit, as described previously [17]. Briefly, in a flat-bottomed 96-well plate 5×10^3 VECs were cultured alone in EBM-2 basal medium (Lonza, USA), with growth factors [5% FBS, VEGF, FGF, EGF, IGF] (EGM-2MV endothelial cell growth medium; Lonza, USA) or with 1×10^5 stimulated mast cells (stimulated with 1 ng/ml IL-33 for 24 hrs) for 24 hours at 37°C. BrdU label was added after 24 hours to each well and incubated for an extra 12 hours at 37°C. Subsequently, the culture plate was processed according to the manufacturer's protocol. A SpectraMax Plus 384 Microplate Reader (Molecular Devices, San Jose, CA, USA) was used to measure absorbance at 450/550 nm.

Real-Time PCR

RNeasy Micro Kits (Qiagen, Valencia, CA, USA) were used to isolate total RNA, as described previously[24]. In brief, purified RNA was reverse transcribed into cDNA using Superscript III (Invitrogen, Carlsbad, CA, USA). Quantitative real-time PCR was conducted using Taqman Universal PCR Mastermix and preformulated primers for murine VEGF-A (Mm00437304_m1) and glyceraldehyde-3-phosphate dehydrogenase (GAPDH, Mm99999915_gl) in a Mastercycler Realplex 2 (Eppendorf, Hamburg, Germany). The comparative threshold cycle method was used to analyze the results, which were normalized to GAPDH as an internal control.

ELISA

Commercially available ELISA kits (R&D Systems, Minneapolis, MN, USA) were used to quantify levels of VEGF-A in lysates of resting or stimulated bone marrow-derived mast cells (stimulated with 1 ng/ml IL-33 for 24 hrs) as per the manufacturer's instructions [25]. Exposure to ethylenediaminetetraacetic acid (EDTA) at 37° C for 30 minutes was used to separate the epithelial layer from the corneas harvested from naïve BALB/c mice. Lysates of corneal epithelial cells served as controls.

Flow Cytometry

Single-cell suspensions were stained with fluorochrome-conjugated anti-CD45, anti-CD11b, anti-cKit, and anti-FcεR1 antibodies. Appropriate isotypes were utilized as antibody

controls. Antibodies and isotype controls were acquired from Biolegend (San Diego, CA, USA). LSR II flow cytometer (BD Biosciences, San Jose, CA, USA) and Summit software (Dako Colorado, Inc., Fort Collins, CO, USA) were used to acquire and analyze stained cells.

β-hexosaminidase Assays

β-n-acetylglucosaminidase assay kits (Sigma-Aldrich) were used to quantify the levels of β-hexosaminidase enzyme. The kit measures the level of 4-Nitrophenyl N-acetyl-β-d-glucosaminide (NP-GlcNAc) hydrolysis [26]. In brief, ocular surface tears were incubated with 0.1 mg/mL NP-GlcNAc (substrate) for 1 hour at 37°C. Subsequently, the enzyme-substrate reaction was stopped with 5 mg/mL sodium carbonate. A SpectraMax Plus 384 Microplate Reader (Molecular Devices, San Jose, CA, USA) was used to measure absorbance at 405 nm. β-hexosaminidase levels were estimated using the formula: U/mL = (A405sample – A405blank) × 0.05 × 0.3 × DF/A405standard × time × volume of sample in milliliters.

Tryptase Assays

Mast Cell Degranulation Assay Kits (Sigma-Aldrich) were used to quantify levels of tryptase enzyme. The kit detects the chromophore p-nitroaniline (pNA) cleaved from the labeled substrate tosyl-gly-pro-lys-pNA [27]. In brief, the ocular surface tear wash was incubated with 0.1 mg/mL tosyl-gly-pro-lys-pNA (substrate) for 3 hours at 37°C. A SpectraMax Plus 384 Reader (Molecular Devices, San Jose, CA, USA) was used to quantify free pNA at 405 nm.

Immunohistochemistry

Corneas with limbus were harvested and immunostained, as previously described [28–30]. Briefly, corneal stroma and epithelium were separated after EDTA treatment for 30 minutes at 37°C, and the stroma was fixed using 4% paraformaldehyde. Tissues were incubated at 4°C with Texas red-conjugated Avidin (ThermoFisher) for 6 hours and FITC-conjugated CD31 (Biolegend) overnight. Stained corneas were whole-mounted on slides and visualized using a confocal microscope (Leica TCS-SP5; Buffalo Grove, IL, USA). The area covered by blood vessel ($CD31^+$) was calculated using ImageJ 1.52s software [17].

Slit-lamp microscopy

Slit-lamp biomicroscopy (with photographs) was used to clinically evaluate corneal neovascularization following suture placement [17]. The slit-lamp analysis was performed on day 2 and 4 post-suture placement. Slit-lamp photographs were converted into binary images, and vascular density as percent area of the vessels in the total cornea was calculated using the ‘Vessel analysis’ plugin in ImageJ 1.52S.

Statistical Analysis

Unpaired two-tailed Student t-tests were used to compare means between two groups. The significance level was set at $p < 0.05$. Data are presented as the mean ± standard deviation. Results shown are representative of at least three independent experiments.

Results

Activation of ocular surface mast cells during suture-induced corneal neovascularization

To evaluate the distribution of mast cells at the ocular surface, we harvested naïve cornea and immunostained with fluorochrome-conjugated avidin, which specifically binds to mast cells [31]. The whole-mount analysis showed that mast cells were distributed along the corneal periphery in the limbal area (Fig. 1A). To further analyze mast cell distribution in conjunction with blood vessels, naïve and sutured corneas were stained with a fluorescent conjugate of avidin and CD31. We employed a model of inflammatory corneal neovascularization by placing a single intrastromal figure-of-eight suture 1 mm from the limbus [17]. Similar to previous studies, we see increased infiltration of immune cells following suture placement (Fig. S2). Mast cells were primarily located near the limbal blood vessels at naïve state and migrated centrally into the cornea alongside the new blood vessel growth (Fig. 1B). At 6 hours post-suture placement, corneas were harvested, and single-cell suspensions were stained withed fluorochrome-conjugated CD11b, c-Kit, and FCεR1 monoclonal antibodies. Flow cytometric quantification analysis further confirmed increased frequencies of cKit+FCεR1+ mast cells following suture placement (Fig. 1C). Tear wash was collected within 6 hours of suture placement for tryptase and β-hexosaminidase analysis, measures of mast cell activation [32]. Naïve mice were used as controls. Our data demonstrated a significant increase in both tryptase and β-hexosaminidase in the tear wash following suture placement (5-fold increase [p=0.008] and 2.5 fold increase [p=0.004], respectively) (Fig. 1D). Next, to investigate the pathway involved in neovascularization following suture placement, we harvested corneas at 6 hours post-suture and evaluated the expression of vascular endothelial growth factor A (VEGF-A) using real-time PCR. Our data showed a substantial increase in VEGF-A expression following suture placement, relative to naïve controls ($p = 0.0001$) (Fig. 1E). Our data demonstrate that during suture-induced corneal neovascularization, mast cells are activated and infiltrate the cornea in close association with new blood vessels.

Deficiency of mast cells reduces corneal neovascularization

Having observed increased frequencies of activated mast cells during corneal neovascularization, we sought to investigate whether mast cells promote the generation of new blood vessels. To assess this, we induced corneal neovascularization in mast cell-deficient mice ($cKit^{w\text{-}sh}$), with wild type C57BL/6 mice as controls. We clinically assessed neovascularization every 2 days post-suture using a slit-lamp biomicroscope (Fig. 2A). Slit-lamp images were converted into binary images using ImageJ software to quantify vascular density, which measures the percent area of the cornea covered by blood vessels. Significantly less corneal neovascularization was observed in $cKit^{w\text{-}sh}$ mice on day 4 compared to WT mice ($p=0.0003$; Fig. 2B). To observe small vessel growth, not visible to the naked eye, corneas were harvested on day 4 post-suture and immunostained with fluorochrome-conjugated CD31. Blood vessel growth was quantitatively analyzed by calculating the neovascular area, the area covered by branching blood vessels, using ImageJ software. Consistent with the clinical observation, $cKit^{w\text{-}sh}$ mice showed significantly less corneal neovascularization compared to WT mice ($p=0.009$; Fig. 2C). WT and $cKit^{w\text{-}sh}$ mice showed no difference in baseline limbal blood vessel area. Furthermore, corneas were

harvested, and the expression of VEGF-A was evaluated using real-time PCR. Naïve corneas of each mice served as the respective baseline. A significantly higher increase in VEGF-A expression was observed in WT mice (6.2-fold) compared to $cKit^{w\text{-}sh}$ mice (2-fold) ($p=0.009$; Fig. 2D). These data suggest that mast cells are critical in promoting corneal neovascularization.

Mast cells directly promote proliferation and tube formation of vascular endothelial cells

To investigate whether the increase of VEGF-A expression following suture placement is due to mast cells, we evaluated the expression of VEGF-A by mast cells. Corneal epithelial cells were used as control. Bone marrow-derived mast cells (purity ≥90%; Fig. S1) were stimulated for 24 hours with IL-33, a known mast cell activator [33], that was significantly upregulated in the cornea following suture placement (Fig. S3) [34]. Lysates of stimulated mast cells showed higher mRNA expression of VEGF-A compared to resting mast cells (Fig. 3A). Compared to corneal epithelial cells as control cells that did not express detectable protein levels of VEGF-A, mast cells expressed high levels of VEGF-A, as shown by the ELISA analysis (Fig. 3B).

Next, to determine whether mast cells can directly promote hemangiogenesis, we conducted an *in vitro* co-culture of mast cells and vascular endothelial cells (VECs). Simulated mast cells were co-cultured with VECs on a gel matrix, and tube formation was observed using a brightfield microscope. At 12 hours of co-culture, VECs co-cultured with mast cells showed a significantly higher tube formation compared to VECs cultured in basal media. In fact, mast cells stimulated VEC tube formation was comparable to that of VECs cultured with known vascular endothelial growth factors (5% FBS, VEGF, FGF, EGF, IGF) (Fig. 3C). To quantify tube formation, brightfield images were analyzed using the ‘Angiogenesis Analyzer’ plugin in ImageJ software. VECs co-cultured with mast cells resulted in significantly more branch and node formation ($p=0.002$ and $p=0.007$, respectively) as well as higher total branch length ($p=0.01$; measures of tube formation) compared to VECs cultured in basal media (Fig. 3D). Consistent with the tube formation data, VECs showed a significant increase in proliferation when co-cultured with mast cells ($p\leq0.0001$; Fig. 3E). Collectively, our data indicate that mast cells secrete high levels of VEGF-A and promote tube formation and proliferation of vascular endothelial cells.

Pharmacological inhibition of mast cell activation suppresses corneal neovascularization

Finally, to assess whether inhibiting mast cell activation prevents corneal neovascularization, we treated sutured corneas with a known mast cell inhibitor (2% cromolyn) [35]. We have previously shown that topical treatment with cromolyn effectively suppresses ocular surface mast cell activation in a murine model of corneal inflammation [13, 14]. Corneas were treated five times a day as outlined in the experimental design, and PBS served as a control (Fig. 4A).

Corneal neovascularization was clinically assessed every 2 days using a slit-lamp biomicroscope (Fig. 4B). Binary images from slit-lamp photographs were created to quantify vascular density using the ImageJ software. Cromolyn treatment resulted in significantly less neovascularization compared to the PBS treatment on day 4 ($p=0.04$; Fig.

4C). To further confirm the inhibitory effect of cromolyn on corneal neovascularization, corneas were harvested on day 4 for immunohistochemistry analysis. Similar to clinical observation, cromolyn-treated corneas showed significantly smaller vessel area relative to the PBS treated controls ($p=0.005$; Fig.4D). Taken together, these results suggest blockade of mast cell activation suppresses corneal neovascularization.

Discussion

This study advances our understanding of the contribution of mast cells to ocular angiogenesis. Mast cell-deficient mice ($cKit^{w\text{-}sh}$ mice) develop significantly less corneal neovascularization, demonstrating for the first time that ocular surface mast cells are critical for corneal angiogenesis. In addition, we show that mast cells: (i) are activated and infiltrate into the cornea in conjunction with new blood vessel growth following corneal suture placement, (ii) secrete high levels of VEGF-A, and (ii) directly promote tube formation and proliferation of vascular endothelial cell proliferation. Lastly, we demonstrate that corneal neovascularization can be suppressed by pharmacologically inhibiting the activation of mast cells at the ocular surface.

Mast cells, characterized by the numerous granules in their cytoplasm, are known for their role in initiating IgE-mediated allergic response by secreting preformed inflammatory mediators [36]. Apart from their well-characterized role in allergic inflammation, mast cells have been implicated in a wide range of pathological conditions, including angiogenesis [6]. Angiogenesis, also known as neovascularization, is the formation of new blood vessels from parental vessels [37]. Although neovascularization can be physiological, uncontrolled angiogenesis has been associated with excessive inflammation and tumor growth [4]. A clinical observational study has observed a higher number of mast cells correlate with gastric carcinoma malignancy grade and the extent of tumor angiogenesis [38]. However, the majority of research on mast cells in pathological angiogenesis has been limited to the tumor microenvironment [15, 39]. Our study expands the current knowledge by demonstrating the role of mast cells in promoting pathological neovascularization at the ocular surface.

Consistent with previous observations, we show that mast cells are primarily located around the limbus in the cornea [6, 13]. Following corneal suture placement, a murine model of corneal neovascularization, we observe increased expression of inflammatory moleculess known to activate mast cells, including IL-33 and Substance P, which have also been shown to regulate corneal neovascularization [40, 41]. Significantly higher frequencies of mast cells infiltrate the cornea and migrate into the central cornea alongside the newly formed vessels. Moreover, we demonstrate enhanced mast cell activation in sutured corneas compared to naïve controls. Corroborating the close association of mast cell activation and corneal neovascularization, we observe significantly less vessel growth in mast cell-deficient $cKit^{w\text{-}sh}$ mice following suture placement compared to the wild type control. Based on these observations, we postulated that ocular surface mast cells directly promote neovascularization.

VEGF-A, a primary member of the VEGF family, is a potent pro-angiogenic factor that mediates angiogenesis by promoting endothelial cell growth, migration, and by inhibiting

apoptosis [42]. Although a previous study has shown that mast cells secrete VEGF-A, the finding was limited to IgE-dependent activation [43]. We demonstrate for the first time that non-IgE mediated activation of mast cells also results in enhanced VEGF-A expression. Furthermore, we demonstrate that vascular endothelial cells co-cultured with mast cells result in more tube formation. In addition, our data show that mast cells directly induce vascular endothelial cell proliferation. Taken together, our findings suggest that mast cells directly promote proliferation and tube formation of vascular endothelial cells by secreting high levels of VEGF-A.

Cromolyn sodium, a mast cell inhibitor, is widely used in the clinic to manage allergy symptoms. The 2% cromolyn sodium eye drops are an effective treatment for allergic conjunctivitis [44]. Moreover, we have previously demonstrated that the topical application of cromolyn effectively inhibits mast cell activation during non-allergic tissue inflammation [13, 14]. To evaluate whether inhibiting mast cell activation leads to less corneal neovascularization, we treated sutured corneas with cromolyn sodium. In the cromolyn treatment group, we observe significantly less corneal neovascularization compared to the PBS treated group.

In summary, our data provide novel insights on the role of ocular surface mast cells in corneal neovascularization. Mast cells, which secrete high levels of VEGF-A, induce vascular endothelial cell proliferation and new vessel formation. Finally, we report that pharmacological inhibition of ocular surface mast cells suppresses corneal neovascularization, suggesting mast cells could be a potential therapeutic target for treating corneal neovascularization.

Supplementary Material

Refer to Web version on PubMed Central for supplementary material.

References

[1]. Ellenberg D, Azar DT, Hallak JA, Tobaigy F, Han KY, Jain S, et al. Novel aspects of corneal angiogenic and lymphangiogenic privilege. Prog Retin Eye Res. 2010;29:208–48.10.1016/j.preteyeres.2010.01.002 [PubMed: 20100589]

[2]. Chang JH, Gabison EE, Kato T, Azar DT. Corneal neovascularization. Current opinion in ophthalmology. 2001;12:242–9.10.1097/00055735-200108000-00002 [PubMed: 11507336]

[3]. Maddula S, Davis DK, Maddula S, Burrow MK, Ambati BK. Horizons in therapy for corneal angiogenesis. Ophthalmology. 2011;118:591–9.10.1016/j.ophtha.2011.01.041 [PubMed: 21376242]

[4]. Aguilar-Cazares D, Chavez-Dominguez R, Carlos-Reyes A, Lopez-Camarillo C, Hernadez de la Cruz ON, Lopez-Gonzalez JS. Contribution of Angiogenesis to Inflammation and Cancer. Front Oncol. 2019;9:1399-.10.3389/fonc.2019.01399 [PubMed: 31921656]

[5]. Elshabrawy HA, Chen Z, Volin MV, Ravella S, Virupannavar S, Shahrara S. The pathogenic role of angiogenesis in rheumatoid arthritis. Angiogenesis. 2015;18:433–48.10.1007/s10456-015-9477-2 [PubMed: 26198292]

[6]. Norrby K Mast cells and angiogenesis. APMIS : acta pathologica, microbiologica, et immunologica Scandinavica. 2002;110:355–71.10.1034/j.1600-0463.2002.100501.x

[7]. Liu J, Fu T, Song F, Xue Y, Xia C, Liu P, et al. Mast Cells Participate in Corneal Development in Mice. Scientific reports. 2015;5:1756910.1038/srep17569 [PubMed: 26627131]

[8]. Metcalfe DD, Baram D, Mekori YA. Mast cells. Physiological reviews. 1997;77:1033–79.10.1152/physrev.1997.77.4.1033 [PubMed: 9354811]

[9]. Wernersson S, Pejler G. Mast cell secretory granules: armed for battle. Nature reviews Immunology. 2014;14:478–94.10.1038/nri3690

[10]. Galli SJ, Kalesnikoff J, Grimbaldeston MA, Piliponsky AM, Williams CM, Tsai M. Mast cells as "tunable" effector and immunoregulatory cells: recent advances. Annual review of immunology. 2005;23:749–86.10.1146/annurev.immunol.21.120601.141025

[11]. Khazaie K, Blatner NR, Khan MW, Gounari F, Gounaris E, Dennis K, et al. The significant role of mast cells in cancer. Cancer metastasis reviews. 2011;30:45–60.10.1007/s10555-011-9286-z [PubMed: 21287360]

[12]. Hueber AJ, Asquith DL, Miller AM, Reilly J, Kerr S, Leipe J, et al. Mast cells express IL-17A in rheumatoid arthritis synovium. Journal of immunology (Baltimore, Md : 1950). 2010;184:3336–40.10.4049/jimmunol.0903566

[13]. Li M, Mittal SK, Foulsham W, Amouzegar A, Sahu SK, Chauhan SK. Mast cells contribute to the induction of ocular mucosal alloimmunity. American journal of transplantation : official journal of the American Society of Transplantation and the American Society of Transplant Surgeons. 2019;19:662–73.10.1111/ajt.15084

[14]. Sahu SK, Mittal SK, Foulsham W, Li M, Sangwan VS, Chauhan SK. Mast Cells Initiate the Recruitment of Neutrophils Following Ocular Surface Injury. Investigative ophthalmology & visual science. 2018;59:1732–40.10.1167/iovs.17-23398 [PubMed: 29610857]

[15]. Ribatti D, Crivellato E. Mast cells, angiogenesis, and tumour growth. Biochimica et Biophysica Acta (BBA) - Molecular Basis of Disease. 2012;1822:2–8.10.1016/j.bbadis.2010.11.010 [PubMed: 21130163]

[16]. Coussens LM, Raymond WW, Bergers G, Laig-Webster M, Behrendtsen O, Werb Z, et al. Inflammatory mast cells up-regulate angiogenesis during squamous epithelial carcinogenesis. Genes & development. 1999;13:1382–97.10.1101/gad.13.11.1382 [PubMed: 10364156]

[17]. Chauhan SK, Jin Y, Goyal S, Lee HS, Fuchsluger TA, Lee HK, et al. A novel prolymphangiogenic function for Th17/IL-17. Blood. 2011;118:4630–4.10.1182/blood-2011-01-332049 [PubMed: 21908425]

[18]. Jin Y, Chauhan SK, El Annan J, Annan JE, Sage PT, Sharpe AH, et al. A novel function for programmed death ligand-1 regulation of angiogenesis. The American journal of pathology. 2011;178:1922–9.10.1016/j.ajpath.2010.12.027 [PubMed: 21435468]

[19]. Saban DR, Bock F, Chauhan SK, Masli S, Dana R. Thrombospondin-1 derived from APCs regulates their capacity for allosensitization. Journal of immunology (Baltimore, Md : 1950). 2010;185:4691–7.10.4049/jimmunol.1001133

[20]. Mittal SK, Foulsham W, Shukla S, Elbasiony E, Omoto M, Chauhan SK. Mesenchymal Stromal Cells Modulate Corneal Alloimmunity via Secretion of Hepatocyte Growth Factor. Stem cells translational medicine. 2019;8:1030–40.10.1002/sctm.19-0004 [PubMed: 31179638]

[21]. Jin Y, Chauhan SK, El Annan J, Annan JEI, Sage PT, Sharpe AH, et al. A novel function for programmed death ligand-1 regulation of angiogenesis. Am J Pathol. 2011;178:1922–9.10.1016/j.ajpath.2010.12.027 [PubMed: 21435468]

[22]. LeCouter J, Kowalski J, Foster J, Hass P, Zhang Z, Dillard-Telm L, et al. Identification of an angiogenic mitogen selective for endocrine gland endothelium. Nature. 2001;412:877–84.10.1038/35091000 [PubMed: 11528470]

[23]. Chauhan SK, Lee HK, Lee HS, Park EY, Jeong E, Dana R. PTK7+ Mononuclear Cells Express VEGFR2 and Contribute to Vascular Stabilization by Upregulating Angiopoietin-1. Arterioscler Thromb Vasc Biol. 2015;35:1606–15.10.1161/ATVBAHA.114.305228 [PubMed: 25997931]

[24]. Shukla S, Mittal SK, Foulsham W, Elbasiony E, Singhania D, Sahu SK, et al. Therapeutic efficacy of different routes of mesenchymal stem cell administration in corneal injury. The ocular surface. 2019;17:729–36.10.1016/j.jtos.2019.07.005 [PubMed: 31279065]

[25]. Mittal SK, Mashaghi A, Amouzegar A, Li M, Foulsham W, Sahu SK, et al. Mesenchymal Stromal Cells Inhibit Neutrophil Effector Functions in a Murine Model of Ocular Inflammation. Investigative ophthalmology & visual science. 2018;59:1191–8.10.1167/iovs.17-23067 [PubMed: 29625439]

[26]. Wolf AJ, Reyes CN, Liang W, Becker C, Shimada K, Wheeler ML, et al. Hexokinase Is an Innate Immune Receptor for the Detection of Bacterial Peptidoglycan. Cell. 2016;166:624–36.10.1016/j.cell.2016.05.076 [PubMed: 27374331]

[27]. Summers SA, Gan PY, Dewage L, Ma FT, Ooi JD, O'Sullivan KM, et al. Mast cell activation and degranulation promotes renal fibrosis in experimental unilateral ureteric obstruction. Kidney international. 2012;82:676–85.10.1038/ki.2012.211 [PubMed: 22673890]

[28]. Ferrari G, Hajrasouliha AR, Sadrai Z, Ueno H, Chauhan SK, Dana R. Nerves and neovessels inhibit each other in the cornea. Investigative ophthalmology & visual science. 2013;54:813–20.10.1167/iovs.11-8379 [PubMed: 23307967]

[29]. Chung ES, Saban DR, Chauhan SK, Dana R. Regulation of blood vessel versus lymphatic vessel growth in the cornea. Investigative ophthalmology & visual science. 2009;50:1613–8.10.1167/iovs.08-2212 [PubMed: 19029028]

[30]. Lee HS, Chauhan SK, Okanobo A, Nallasamy N, Dana R. Therapeutic efficacy of topical epigallocatechin gallate in murine dry eye. Cornea. 2011;30:1465–72.10.1097/ICO.0b013e31821c9b5a [PubMed: 21993466]

[31]. Bergstresser PR, Tigelaar RE, Tharp MD. Conjugated avidin identifies cutaneous rodent and human mast cells. The Journal of investigative dermatology. 1984;83:214–8.10.1111/1523-1747.ep12263584 [PubMed: 6470526]

[32]. Moon TC, Befus AD, Kulka M. Mast cell mediators: their differential release and the secretory pathways involved. Front Immunol. 2014;5:56910.3389/fimmu.2014.00569 [PubMed: 25452755]

[33]. Elbasiony E, Mittal SK, Foulsham W, Cho W, Chauhan SK. Epithelium-derived IL-33 activates mast cells to initiate neutrophil recruitment following corneal injury. . Ocular Surface. 2020;18:633–40. 10.1016/j.jtos.2020.06.006 [PubMed: 32615259]

[34]. Saluja R, Ketelaar ME, Hawro T, Church MK, Maurer M, Nawijn MC. The role of the IL-33/IL-1RL1 axis in mast cell and basophil activation in allergic disorders. Molecular immunology. 2015;63:80–5.10.1016/j.molimm.2014.06.018 [PubMed: 25017307]

[35]. Altounyan RE. Review of clinical activity and mode of action of sodium cromoglycate. Clinical allergy. 1980;10 Suppl:481–9.10.1111/j.1365-2222.1980.tb02162.x [PubMed: 6821510]

[36]. Galli SJ, Tsai M. IgE and mast cells in allergic disease. Nat Med. 2012;18:693–704.10.1038/nm.2755 [PubMed: 22561833]

[37]. Feizi S, Azari AA, Safapour S. Therapeutic approaches for corneal neovascularization. Eye Vis (Lond). 2017;4:28-.10.1186/s40662-017-0094-6 [PubMed: 29234686]

[38]. Ribatti D, Guidolin D, Marzullo A, Nico B, Annese T, Benagiano V, et al. Mast cells and angiogenesis in gastric carcinoma. Int J Exp Pathol. 2010;91:350–6.10.1111/j.1365-2613.2010.00714.x [PubMed: 20412338]

[39]. Soucek L, Lawlor ER, Soto D, Shchors K, Swigart LB, Evan GI. Mast cells are required for angiogenesis and macroscopic expansion of Myc-induced pancreatic islet tumors. Nat Med. 2007;13:1211–8.10.1038/nm1649 [PubMed: 17906636]

[40]. Barbariga M, Fonteyne P, Ostadreza M, Bignami F, Rama P, Ferrari G. Substance P Modulation of Human and Murine Corneal Neovascularization. Investigative ophthalmology & visual science. 2018;59:1305–12.10.1167/iovs.17-23198 [PubMed: 29625453]

[41]. Theodoropoulou S, Copland DA, Liu J, Wu J, Gardner PJ, Ozaki E, et al. Interleukin-33 regulates tissue remodelling and inhibits angiogenesis in the eye. The Journal of pathology. 2017;241:45–56.10.1002/path.4816 [PubMed: 27701734]

[42]. Holmes DIR, Zachary I. The vascular endothelial growth factor (VEGF) family: angiogenic factors in health and disease. Genome Biol. 2005;6:209-.10.1186/gb-2005-6-2-209 [PubMed: 15693956]

[43]. Boesiger J, Tsai M, Maurer M, Yamaguchi M, Brown LF, Claffey KP, et al. Mast cells can secrete vascular permeability factor/ vascular endothelial cell growth factor and exhibit enhanced release after immunoglobulin E-dependent upregulation of fc epsilon receptor I expression. The Journal of experimental medicine. 1998;188:1135–45.10.1084/jem.188.6.1135 [PubMed: 9743532]

[44]. Kray KT, Squire EN Jr., Tipton WR, Selner JC, O'Dea J, Nelson HS. Cromolyn sodium in seasonal allergic conjunctivitis. The Journal of allergy and clinical immunology. 1985;76:623–7.10.1016/0091-6749(85)90785-7 [PubMed: 3932499]

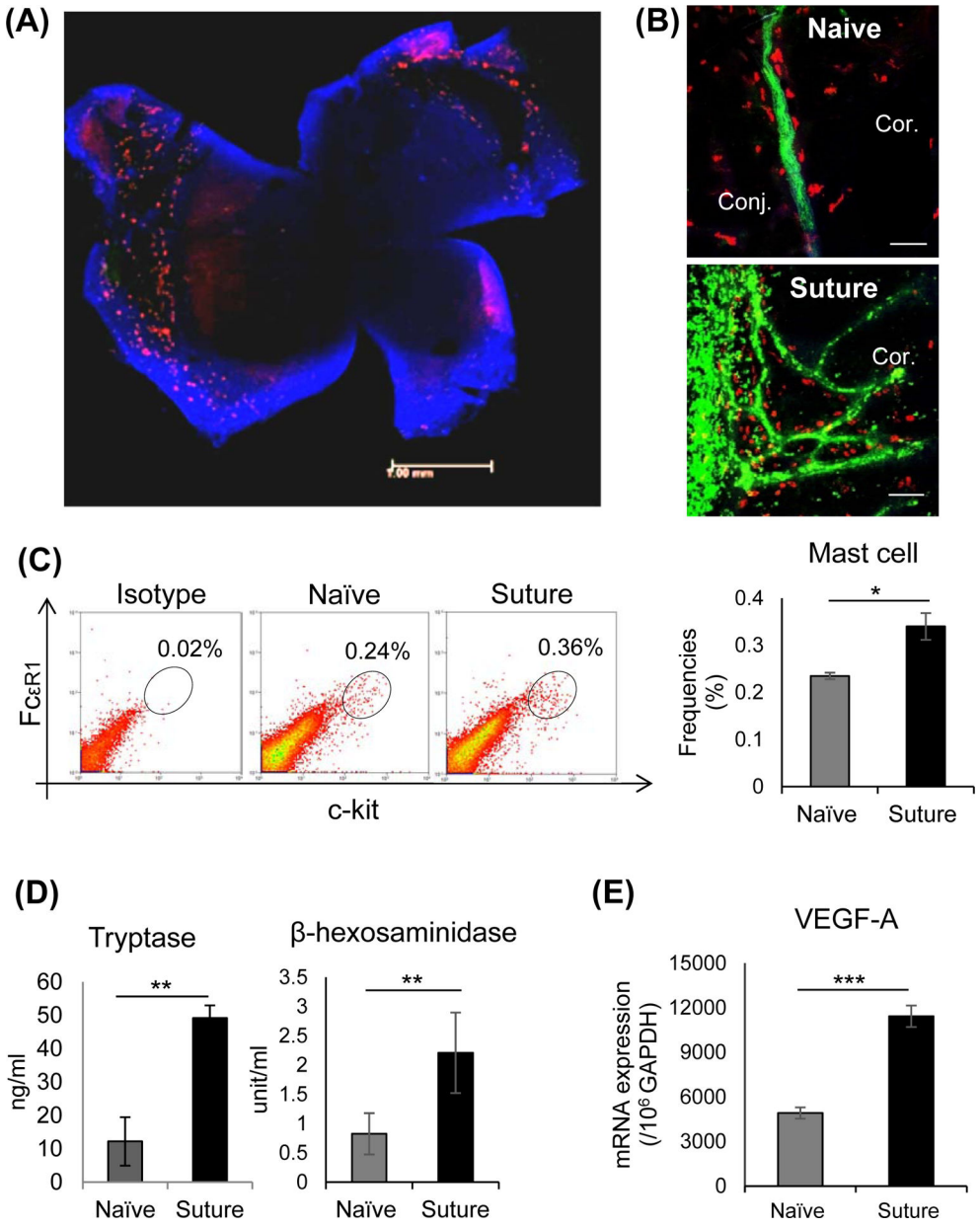

Figure 1. Suture-induced corneal neovascularization activates ocular surface mast cells

(A) Representative immunohistochemistry micrograph of Balb/c murine cornea whole-mounted and stained with fluorescein-conjugated avidin (Texas Red) to visualize mast cells. (B) Representative immunohistochemistry micrographs of mast cell (Avidin-Texas red) and blood vessel growth (CD31-FITC) of the murine cornea on day 4 following intrastromal suture placement compared to naïve cornea (Scale bar, 100 μm). (C) Ocular surface mucosal tissues were harvested 6 hours post-suture placement, and single-cell suspensions were prepared for analysis. Representative flow cytometric dot plots (left) and cumulative bar chart (right) showing the frequencies of $CD11b^{-}$-$Kit^{+}FC\varepsilon R1^{+}$ mast cells at ocular surface 6 hrs following corneal suture (Data shown are gated on $CD11b^{-}$cells). (D) Ocular surface tear wash was collected at 0h, 1h, 3h, and 6h following suture placement (5μl/wash) to measure

mast cell activation markers tryptase (left) and β-hexosaminidase (right). (E) Bar chart depicting expression of VEGF-A in the cornea post-suture compared to naïve state, as quantified by real-time PCR. Representative data from three independent experiments are shown, and each experiment consisted of 4 animals per group. Data are represented as mean ± SD (error bar). T-test; *$p<0.05$, **$p < 0.01$, ***$p < 0.001$.

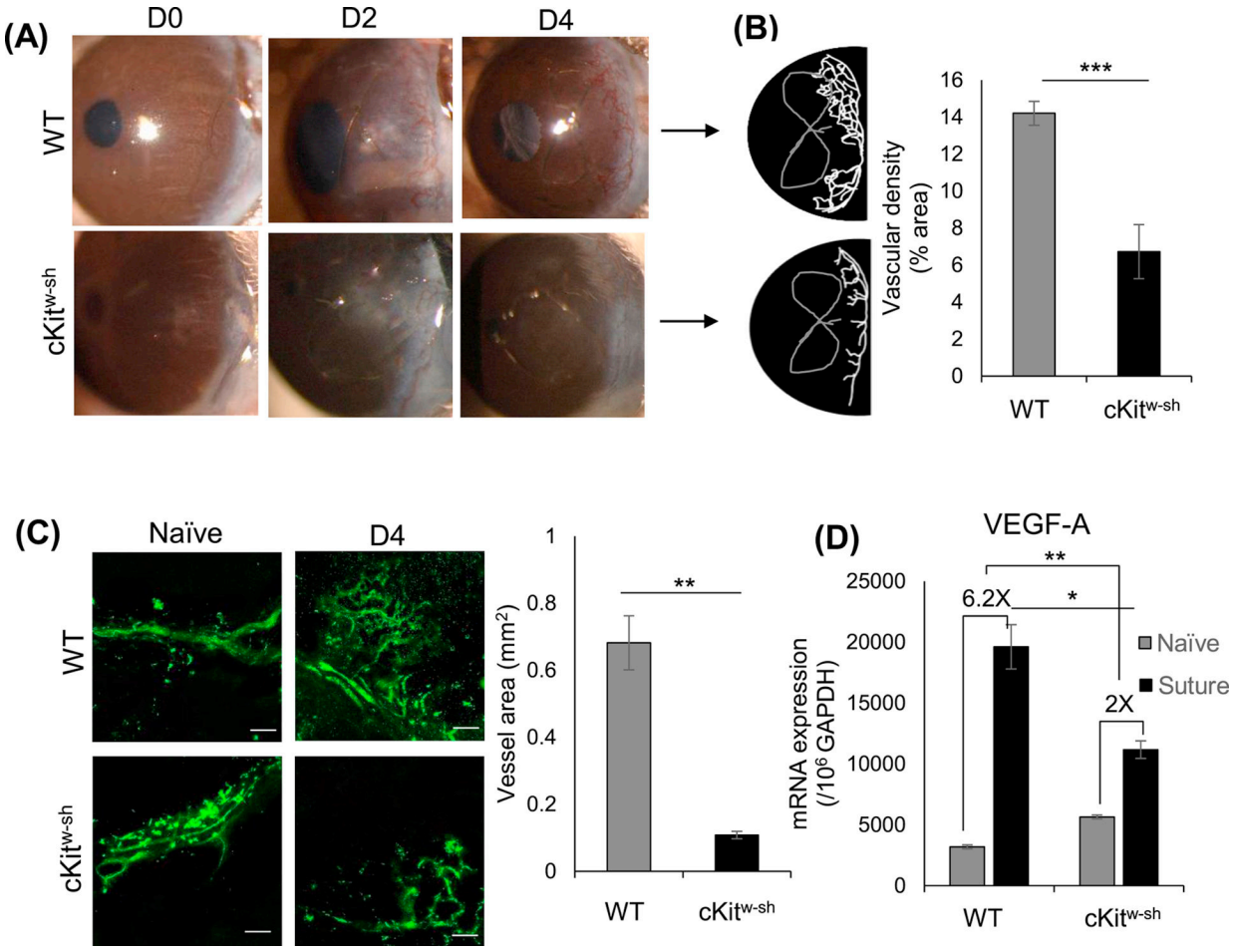

Figure 2. Mast cell-deficient mice develop reduced corneal neovascularization

(A) Representative slit-lamp biomicroscope photographs of naïve and sutured corneas of wild type (C57BL/6) and cKit$^{w\text{-}sh}$ mice on days 0, 2, and 4 post-suture placement. (B) Binary image (left) and cumulative bar chart (right) depicting the vascular density of corneal neovascularization. Slit-lamp photographs were converted into binary images, and vascular density as percent area of the vessels in the total cornea was calculated using the 'Vessel analysis' plugin in ImageJ 1.52S software. (C) Corneas were harvested on day 4 post-suture placement and immunostained with CD31 (FITC). Representative immunohistochemistry micrographs (left) and cumulative bar chart (right) showing vessel area in corneas of WT and cKit$^{w\text{-}sh}$ mice. ImageJ 1.52S software was used to quantify the vessel area (Scale bar, 100 μm). (D) Bar chart depicting expression of VEGF-A in the cornea post-suture compared to naïve state, as quantified by real-time PCR. WT and cKit$^{w\text{-}sh}$ mice showed a 6.2-fold and 2-fold increase in VEGF-A expression post-suture placement, respectively. Representative data from three independent experiments are shown, and each experiment consisted of n = 3 animals/group. Data are represented as mean ± SD (error bar). T-test; *$p < 0.05$, **$p < 0.01$, ***$p < 0.001$.

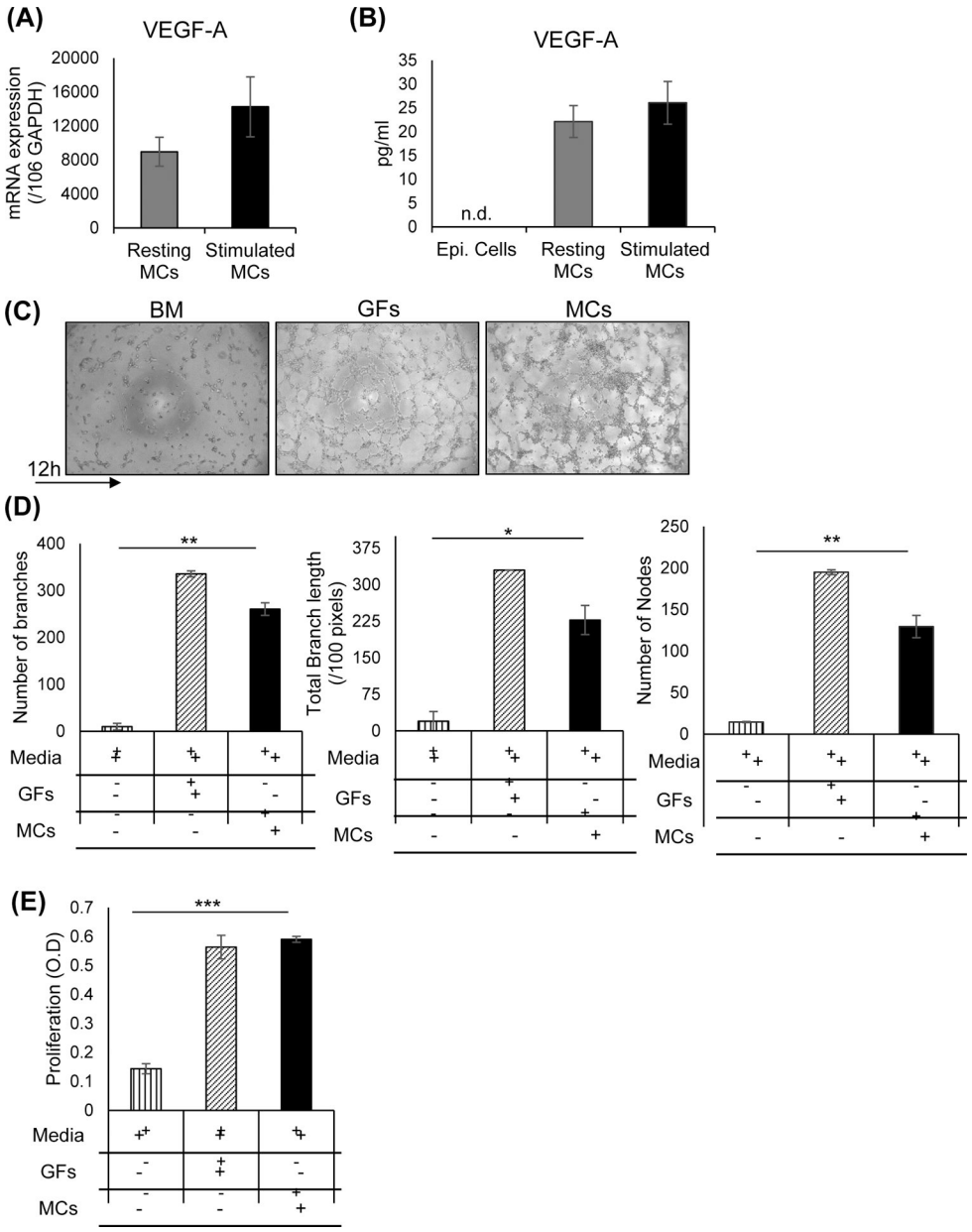

Figure 3. Mast cells express high levels of VEGF-A and promote proliferation and tube formation of vascular endothelial cells

Bone-derived mast cells were cultured in medium alone (Resting mast cells) or stimulated with IL-33 (1 ng/ml) for 24 hours and lysed to quantify (A) mRNA expression of VEGF-A as quantified by real-time PCR and (B) protein levels of VEGF-A as quantified by ELISA. Lysate of corneal epithelium harvested from naïve mice served as a negative control. (C) Representative brightfield micrographs showing tube formation of vascular endothelial cells at 12 hours of indicated co-cultures. Vascular endothelial cells were cultured alone in basal media, with growth factor (GF) supplements or with MCs at 1:1 ratio (stimulated with 1 ng/ml IL-33 for 24 hrs) at 37°C on a gel matrix to measure tube formation. (D) Bar chart showing measures of tube formation (number of branches, total branch length, number of nodes) in the above co-cultures. Tube formation was quantified by analyzing brightfield

micrographs using Angiogenesis Analyzer plugin in ImageJ 1.52s software. (E) Bar chart showing the proliferation of vascular endothelial cells in the indicated co-cultures. VECs were cultured alone in basal media, with growth factor supplements or with stimulated MCs (stimulated with 1 ng/ml IL-33 for 24 hrs) for 36 hours at 37°C, and proliferation was measured using BrdU incorporation assays. Representative data from three independent experiments are shown. Data are represented as mean ± SD (error bar). T-test; *$p < 0.05$, **$p < 0.01$, ***$p < 0.001$. BM, basal media; GFs, growth factors; MCs, mast cells.

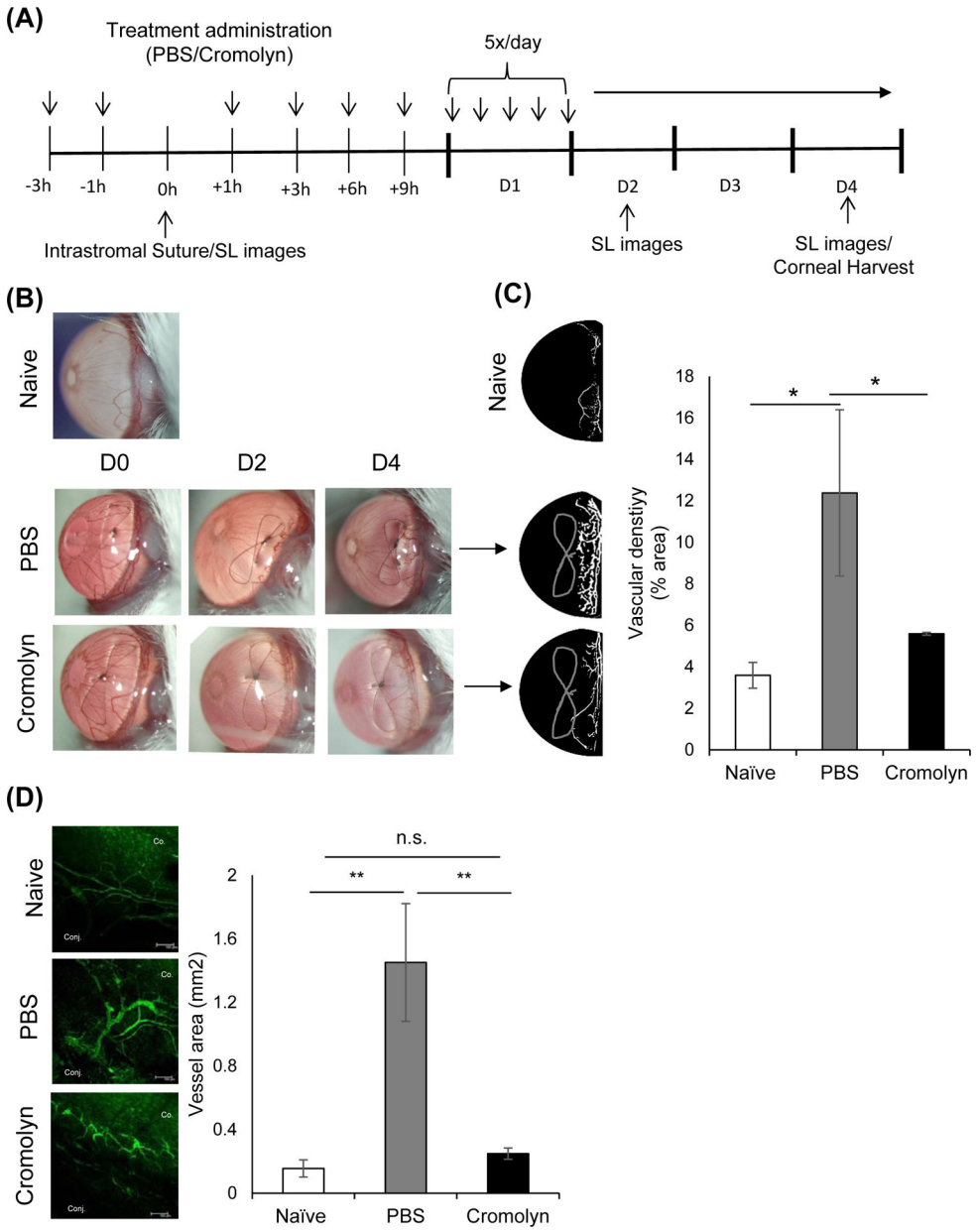

Figure 4. *In vivo* blockade of mast cell activation abates corneal neovascularization

(A) Schematic experiment design showing the time points of treatment administration in mice with intrastromal sutures. Mice were treated with PBS (3 μl/time) or 2% cromolyn (3 μl/time). After 4 days, corneas were harvested for immunohistochemistry analysis of corneal neovascularization. (B) Representative slit lamp biomicroscope photographs of naïve and sutured corneas treated with PBS or cromolyn on day 0, 2 and 4 post-suture placement. (C) Binary images (left) and cumulative bar chart (right) depicting vascular density of corneal neovascularization. Slit-lamp photographs were converted into binary images and vascular density as percent area of the vessels in total cornea was calculated using the 'Vessel analysis' plugin in ImageJ 1.52S software. (D) Representative immunohistochemistry micrographs (left) and cumulative bar chart (right) showing vessel area in naïve and sutured

corneas treated with PBS or cromolyn. Corneas were harvested on day 4 post-suture placement and immunostained with CD31 (FITC). ImageJ 1.52S software was used to quantify the vessel area (Scale bar, 100 μm). Representative data from three independent experiments are shown, and each experiment consisted of four animals. Data are represented as mean ± SEM (error bar). T-test; *$p < 0.05$, **$p < 0.01$, n.s not significant.